International Journal of Science and Research (IJSR)
ISSN (Online): 2319-7064
Index Copernicus Value (2015): 78.96 | Impact Factor (2015): 6.391

Normal Coordinate Analysis, Vibrational Spectroscopy Studies and Quantum Chemical Calculationsof 1,5-Dichloro-2,3-dinitrobenzene

S. Seshadri[1], M. Padmavathy[2]

[1]PG & Research Department of Physics, Head & Associate Professor, UrumuDhanalakshmi College, Kattur, Trichy-620019, India

[2]Department of physics, Shrimati Indira Gandhi College, Trichy-620002, India

Abstract: ***Extensive vibrational investigations of 1,5-Dichloro-2,3-dinitrobenzene (DCDNB) have been carried out with FT-IR and FT-Raman techniques. The electronic structure of the molecule has been analysed by UV-Visible and NMR spectroscopies. This studies were carried out with Hartree-Fock (HF) method utilizing 6-311+G(d,p) and 6-311++G(d,p) basis sets to determine the structural, vibrational and electronic characteristics of the compound. The mixing of the fundamental modes was determined with the help of potential energy distribution (PED).^{13}C and^{1}H NMR chemical shifts and the electronic transitions of the molecule are also discussed.***

Keywords: FT-IR, FT-Raman, NMR, PED, HF

1. Introduction

Nitrobenzene is water insoluble pale yellow oil with an almond like odor. It freezes to give greenish yellow crystals. It is produced on a large scale as a precursor to aniline. Although occasionally used as a flavoring or perfume additive, nitrobenzene is highly toxic in large quantities. In the laboratory, it is occasionally used as a solvent, especially for electrophilic reagents. Nitrobenzene is used mostly in the production of aniline [1], which is a precursor to rubber chemicals, pesticides, dyes, explosives, and pharmaceuticals. 1,2-Dichloro-4-nitrobenzene is a pale yellow solid related to 1,2-dichlorobenzeneby the replacement of one H atom with a nitro functional group. This compound is an intermediate one in the synthesis of agrochemicals. The nitration of 1,2-dichlorobenzene mainly produces 1,2-dichloro-4-nitrobenzene, together with smaller amounts of the 3-nitro isomer. It can also be prepared by chlorination of 4-chloronitrobenzene [1].

Nitrobenzene is also used in shoe and floor polishes, leather dressings, paint solvents and other materials to make unpleasant odors. Redistilled, as oil of mirbane, nitrobenzene is used as an inexpensive perfume for soaps. A significant commercial use of nitrobenzene is its use in the production of the analgesic paracetamol (also known as acetaminophen) (Mannsville 1991) [2]. Apart from its conversion to aniline, nitrobenzene is readily converted to related derivatives such as azobenzene, nitrosobenzene and phenylhydroxylamine. The nitro-group is deactivating and substitution ends to occur at the meta-position. It is also used in the manufacture of azo dyes, fungicides, rubber chemicals and explosives and as an algicide in colant water of air conditioning systems. Therefore an attempt was made to get an insight into the nature of vibrational modes; normal coordinate analysis was performed, which enabled to obtain a detailed interpretation of the vibrational spectra of the DCDNB.

Nitrobenzene can cause a wide variety of harmful health effects to exposed persons. Repeated exposures to a high concentration of nitrobenzene can result in a blood condition called methemoglobinemia (a form of anemia). This condition affects the ability of blood carrying oxygen [3]. Exposure level is extremely high nitrobenzene can cause coma and possibly death unless prompt medical treatment is received. In case of long-term exposure to nitrobenzene, the presence of its breakdown products, p-nitrophenol and p-aminophenol, in the urine is an indication of nitrobenzene exposure. The results of these tests cannot be used to determine the level of nitrobenzene exposure [4,5].

Quantum chemical computational methods have proven to bean essential tool for interpreting and predicting the vibrational spectra [3–6]. A significant advancement in this area was made by combining semi-empirical quantum mechanical method ab initioquantum mechanical method and density functional theory (DFT),each method having its own advantages [5–8]. However, no Fourier transform infrared (FT-IR), (Fourier transform Raman) FT-Raman, ultraviolet visible (UV-Vis)and nuclear magnetic resonance (NMR) analysis using HF method at 6-311++G(d,p) and 6-311+G(d,p)basis sets are reported on DCDNB so far, inspite of its pharmaceutical importance. Hence, in the present work a detailed HF vibrational structure analysis has been attempted by recording FT-IR and FT-Raman spectra of the title compound considering its biological and pharmaceuticaluses.

2. Experimental Details

The fine polycrystalline samples of a 1,5-Dichloro-2,3-dinitrobenzene (DCDNB) was used for the spectral measurements. Fourier transform infrared (FT-IR) spectra of the title compounds are recorded with KBr pellet technique in the 4000–400 cm^{-1} region using BRUKER IFS-66V FT-IR spectrometer equipped with a cooled MCT detector for the mid-IR range at room temperature. The FT-Raman spectrum was recorded on a BRUKER IFS-66Vmodel interferometer equipped with an FRA-106 FT-Raman accessory. The spectrum was recorded in the 3000–100 cm^{-1} stokes region using 1064 nm line of an Nd:YAG laser for

excitation operating at200 mW power. The reported frequencies were accurate, ±1cm^{-1} for FT-IR and FT-Raman. The UV absorption spectrum is registered in ethanol on Shimadzu UV-1800 PC spectrophotometer in the spectral region 800–100 nm.^{13}C and ^{1}H NMR spectra were taken in CDCl3 solutions and all signals were referenced to TMS on a BRUKER TPX-400 FT-NMR spectrometer.

3. Computational Details

The molecular geometry optimization, vibrational frequency calculations were carried out for DCDNB by Gaussian 09W software package [9]using the HF calculations with standard 6-311+G(d,p) and 6-311++G(d,p) basis sets.Initial geometry generated from the standard geometrical parameters was minimized without any constraint on the potential energy distribution at HF level adopting the standard basis sets. All the parameters were allowed to relax and all the calculations converged to an optimized geometry which corresponds to a true minimum, as revealed by the lack of imaginary values in the wavenumber calculations. The Cartesianre presentation of the theoretical force constants have been computed at the fully optimized geometry. The multiple scaling of the force constants were performed according to SQM procedure[10,11]using selective scaling in the natural internal coordinate representation[12, 13]. Transformation of force field, the subsequent normal coordinate analysis including the least square refinement of the scale factors and calculation of the potential energy distribution (PED) were done on a PC with the MOLVIB program (version V7.0-G77) written by Sundius[14, 15]. For the graphs of simulated FT-IR and FT-Raman spectra, pure Lorentzian band shapes were used with a bandwidth of 10 cm^{-1}.

The symmetry of the molecule was also helpful in making vibrational frequencies. The symmetries of the vibrational modes were determined using the standard procedure of transforming the traces of the symmetry operation into irreducible representation. The symmetry analysis for the vibrational modes of DCDNB was done in detail in order to describe the basis for the frequencies. By combining the results of the Gauss view program with symmetry considerations, vibrational frequency analysis were made witha high degree of accuracy. There was always some ambiguity in defining the internal coordinates. However, the defined coordinates form a complete set and match quite well with the motions observed using the Gauss view program.

The Raman activities (S_i) calculated by the Gaussian 09W program was converted to relative Raman intensities (I_i) using the following relationship derived from the intensity theory of Raman scattering [16, 17].

$$I_i = \frac{f(\nu_0 - \nu_i)^4 S_i}{\nu_i[1-\exp(-hc\nu_i / KT)]} \quad (1)$$

where ν_0 is the laser exciting wavenumber in cm^{-1} (in this work, we have used the excitation wavenumber ν_0 = 9398.5 cm^{-1}, which corresponds to the wavelength of 1064 nm of a Nd:YAG laser), ν_i is the vibraional wavenumber of the ith normal mode (cm^{-1}), while S_i is the Raman scattering activity of the normal mode ν_i,f (is a constant equal to 10^{-12}) is a suitably chosen common normalization factor for all peak intensities h, k, c and T are Planck and Boltzmann constants, speed of light and temperature in Kelvin, respectively.

The electronic properties, such as absorption wavelengths and oscillator strengths, reactivity descriptor and ^{13}C NMR and ^{1}H NMR of the title compound have been calculated using HF/6-311+G(d,p) level of theory. Since non-linear optical (NLO) properties, Mulliken charges are calculated at HF method with 6-311+G(d,p) and 6-311++G(d,p) basis sets.

4. Results and Discussion

4.1 Molecular Geometry

The labeling of atoms of DCDNB is shown in Fig. 1. The optimized values of bond lengths, bond angles and dihedral angles are reported in Table 1.The molecule contains two Cland NO2 groups connected with benzene ring. Experimental and simulated spectra of FT-IR and FT-Raman are presented in Figs. 2 and 3,respectively.

From the structural data given in Table 1, it is observed that the various bond lengths and bond angles are found to be almost same at HF/6-311+G(d,p) and HF/6-311++G(d,p) levels. However, the HF/6-311+G(d,p) level of theory, in general slightly over estimates bond lengths and bond angles. The calculated geometric parameters can be used as foundation to calculate the other parameters for the compound.

The optimized molecular structure of DCDNB reveals that the para-substituted nitro group is in planar with the benzene ring. Inclusion of the NO2 group and Cl atoms known for its strong electron-withdrawing nature in para position is expected to increase a contribution of the resonance structure, in which the electronic charge is concentrated at this site. This is the reason for the shortening of bond lengths N8–O9=1.2008 Å, N8–O10=1.347 Å, N11–O12 = 1.3837 Å andN11–O13 = 1.2167 Å obtained by HF/6-311++G(d,p) method. The same bondlengths calculated by HF/6-311+G(d,p) method is found to be 1.2009, 1.3851, 1.3839 and1.2168Å . The carbon atoms are bonded to the hydrogen atoms with an σ-bond in benzene and the substitution of chlorine atoms for hydrogen reduces the electron density at the ring carbon atom. In DCDNB, the C–Cl bond lengths vary from 1.7234, 1.7295Å and 1.7232, 1.7294Å respectively, by HF/6-311+G(d,p) and HF/6-311++G(d,p) levels of theory.

The ring carbon atoms in substituted benzenes exert a larger attraction on the valence electron cloud of the hydrogen atom resulting in an increase in the C–H force constants and a decrease in the corresponding bond length. It is evident from the C–C bond lengths ranging from 1.4627 to 1.3303Å and from 1.4623 to1.3303Å by HF/6-311+G(d,p) and HF/6-311++G(d,p) levels in the benzene ring of DCDNB, whereas the C–H bond lengths in DCDNB for 1.0709, 1.0708 Å and 1.0718, 1.0717 Å by HF method with 6-311+G(d,p) and 6-311++G(d,p) basis sets.The benzene ring appears to be a little distorted because of theNO2 group substitution as seen from the bond angles C1–C2–C3,which are calculated as

116.996˚and 177.040˚, respectively, by same different basis set.

4.2. Vibrational assignments

The DCDNB molecule consists of 16 atoms, which undergoes 42 normal modes of vibrations. On the assumption of C1 group of symmetry, the numbers of vibration modes of the 42 fundamental vibrations of the molecule are distributed as29 in-plane and 13 out-of-plane vibrations of same symmetry species. A detailed description of the vibrational modes can be given by means of normal coordinate analysis(NCA). For this purpose, the full sets of 54 standard internal coordinates (containing 12 redundancies) are defined as given in Table 2. From the full set of 54 internal coordinates, a non-redundant set of local symmetry coordinates are constructed by means of suitable linear combinations of internal coordinates followed by the recommendation of Fogarasi and Pulay [10–12]. The local symmetry co-ordinates corresponding to probable degrees of freedom of DCDNB are presented in Table 3.

The vibrational frequencies calculated at HF level are scaled by 0.905 [18] and the range of wave numbers above 1700 cm^{-1} are scaled as 0.958 and below 1700 cm^{-1} scaled as0.983 for title compound. After scaled with the scaling factor, the deviation from the experiments is less than 10 $cm^{-1}$with a few exceptions. The force fields determined were used to calculate the vibrational potential energy distribution (PED) among the normal coordinates. Finally, the PED for each normal mode among the symmetry coordinates is calculated and given in Table 4.

4.2.1. C–H vibrations

The nitro group does not appear to affect the position of characteristic C–H bands and these bands occur in the range3100–3000cm^{-1}. The in-plane C–H bending vibrations appear in the range 1300–1000 cm^{-1} in the substituted benzenes and the out-of-plane bending vibrations in the range 1000–750 cm^{-1}[19]. The FT-IR vibrational frequencies at 3400(w) and 3250(w) cm^{-1} are assigned to C–H stretching vibrations of DCDNB and show good agreement with the calculated results. The FT-Raman counterparts of C–H stretching vibration is observed at 2750(w) cm^{-1}, which are further supported by the PED contribution of almost 99%.

TheFT-IR bands at 1300 (s), 1250(vs) $cm^{-1}$and FT-Raman bans t 1250(vs) are assigned to C–H in-plane bending vibrations of title molecule. The calculated and observed frequencies of two C–H out-of-plane bending vibrations are occurred within the characteristic region for DCDNB. The observed C–H out-of-plane bending modes show consistent agreement with the computed HF method with 6-311++G(d,p)results.

4.2.2. Nitro (NO2) group vibrations

For molecules with an NO2 group, the NO2 asymmetric stretching vibration band range is 1625–1540 $cm^{-1}$and that of the symmetric stretching vibration is 1400–1360 cm^{-1}[20]. The FT-IR bands are observed at 1950(vw) and 1800(w)cm^{-1}in DCDNB assigned to NO2 asymmetric stretching vibrations. The NO2 symmetric stretching vibrations are observed in FT-IR spectrum at 1600(s) and 1550(w)cm^{-1}.Aromatic nitro compounds have a band of weak-to-medium intensity in the region 590–500 cm^{-1}[20] due to the in-plane deformation (scissoring and rocking) mode of the NO2 group. This was observed at 750(s) and 680(vw)cm^{-1}in FT-Raman spectrum. The deformation vibrations of NO2 group (rocking, wagging and twisting) contribute to several normal modes in the low frequency region [21]. The NO2 wagging vibrations is observed in theFT-Raman spectrum at 400(s) and 300(s) $cm^{-1}$for DCDNB. As the torsion vibrations are very an harmonic, its frequency is difficult to reproduce within the harmonic approach.

4.2.3. C–C vibrations

The ring stretching vibrations are very much important in the spectrum of benzene and its derivatives are highly characteristic of the aromatic ring itself. The ring C–C stretching vibrations, known as semicircle stretching usually occur in the region 1625–1400cm^{-1}[22]. Particularly, the bands between the regions 1650–1590 cm^{-1} [23]and 1590–1430 cm^{-1} [24]in benzene derivatives are usually assigned to C–C and the C–C stretching vibrations, respectively. In the present study, the C–C stretching vibrations are observed at 1700(s) and 1450(vw)cm^{-1} in FT-IR spectrum and 1400(s)cm^{-1} in FT-Raman spectrum. The calculated values are at 1659, 1639, 1439, 1397, 1193and 1152 cm^{-1} by HF/6-311+G(d,p) method and 1651, 1633, 1431, 1396, 1186and 1143 cm^{-1} by HF/6-311++G(d,p).It shows the theoretical values good agreement with experimental data. All the C–C stretching vibrations are observed well below the expected region. From this observation it is clear that the ring stretching vibrations are affected much due to the NO2 and Cl. In the title molecule, the C–C–C out-of-plane bending vibrations are appeared at 650(s) and 510(w)cm^{-1} in FT-IR spectrum and 550(vw) cm^{-1} in FT-Raman spectrum. All the assignments related to in-plane and out-of-plane bending vibrations are in coherent with the literature values [24].

4.2.4 C–N vibrations

In aromatic compounds, the C–N stretching vibration usually lies in the region 1400–1200cm^{-1}. The identification of C–N stretching frequencies is a rather difficult task. Since the mixing of vibrations is possible in this region [23]. In this case, the bands observed at 1150(w) and 1035(vw)cm^{-1} in FT-IR and 1150(w)cm^{-1} in FT-Raman spectra have been assigned to C–N stretching vibrations of DCDNB. The in-plane and out-of-plane bending C–N vibrations have also been identified and these assignments are also supported by the PED values.

4.2.5. C–Cl vibrations

The C–Cl stretching vibrations generally give strong bands in the region of 760–505 cm^{-1}[25]. Vibrational coupling with other vibrational modes may result in a shift in the absorption to as high as 840 cm^{-1}[25]. Based on this, the FT-IR band at 1010(vw) cm^{-1} for DCDNB was within the C–Cl stretching vibration, this was also confirmed by PED output. Most of the aromatic chloro-compounds have a band of strong to medium intensity in the region 385–265 cm^{-1} due to C–Cl in-plane bending vibration [25]. Accordingly, the FT-IR and FT-Raman bands identified at 480(vw) and 250(vw) cm^{-1} for DCDNB were assigned to C–Cl in-plane

bending mode. The C–Cl out-of-plane deformation vibrations were established within the region.

5. Non-Linear Optical (NLO) Properties

The potential application of the DCDNB in the field of non-linear optics demands the investigation of its structural and bonding features contributing to the hyperpolarizability enhancement. For calculating hyperpolarizability, the geometry of the investigated molecule is treated as an isolated molecule. The optimization has been carried out in the unrestricted open-shell HF level. The geometries are fully optimized without any constraint with the help of analytical gradient procedure implemented within Gaussian 09W program [9]. The electric dipole moment and dispersion free first hyperpolarizability are calculated using finite field method. The finite field method offers a straight forward approach to the calculation of hyperpolarizability [26].

In the presence of an applied electric field, first order hyperpolarizability is a third rank tensor that can be described by a 3x3x3 matrix. The components of the 3D matrix can be reduced to 10 components because of the kleinman symmetry [27]. The matrix can be given in the lower tetrahedral format. It is obvious that the lower part of the 3x3x3 matrixes is a tetrahedral.

The total static dipole moment (μ), the average polarizability (α_0) and first hyperpolarizability (β_0) using the x, y, z components they are defined as follows:

$$\mu = \left(\mu_x^2 + \mu_y^2 + \mu_z^2\right)^{1/2} \quad (2)$$

$$\alpha_0 = \frac{1}{3}\left(\alpha_{xx} + \alpha_{yy} + \alpha_{zz}\right) \quad (3)$$

$$\beta_0 = \left[\left(\beta_{xxx} + \beta_{xyy} + \beta_{xzz}\right)^2 + \left(\beta_{yyy} + \beta_{yzz} + \beta_{yxx}\right)^2 + \left(\beta_{zzz} + \beta_{zxx} + \beta_{zyy}\right)^2\right]^{\frac{1}{2}} \quad (4)$$

The $\beta_0$components of Gaussian output are reported in atomic units and therefore the calculated values are converted into esu units (1 a.u=8.3693×10^{-33}esu). The calculated values of hyperpolarizability and polarizability using HF method with 6-311+G(d,p) and 6-311++G(d,p) basis sets are tabulated in Table 5. According to the present calculations, the total molecular dipole moment (μ=23.79 and 23.54 Debye), average polarizability (α_0=–99.413×$10^{-24}$and 99.313×10^{-24}esu) and the first hyperpolarizability (β_0=1.668×$10^{-24}$and 1.662×10^{-24}esu) for DCDNB molecule using HF method with 6-31+G(d,p) and 6-31++G(d,p) basis sets.

6. Mulliken Atomic Charges

The charge distribution on the molecule has an important influence on the vibrational spectra. The calculated Mulliken [28] charge distributions of benzene derivates are compared in Table 6. The results show that substitution of the aromatic ring by NO2 groups and chlorine atoms leads to a redistribution of electron density. The corresponding Mulliken's plot is shown in Fig. 4.The results show that substitution of the aromatic ring by Cl atom leads to a redistribution of electron density of benzene. As can be seen in Table 6,all the hydrogen atoms have a net positive charge in both basis sets. Moreover, for Chlorine benzene molecule accommodate higher positive charge than the hydrogen atoms. For nitrobenzene, oxygen atoms accommodate higher positive charge than the H14 and H16hydrogen atoms. This is due to the presence of electronegative chlorine atom, the hydrogen atom attract the positive charge from the chlorine atom.

7. Reactive Descriptors

Global reactivity parameters

The frontier electron theory of chemical reactivity can be rationalized from DFT study of the electronic structure [29].The electron density distribution is the fundamental concept for understanding the chemical reactivity and can explain the phenomena nucleophilic, electrophilic and free radical attacks on molecules. For a system of N electrons with ground state energy E (n, v), where v is the potential energy acting on an electron due to presence of all nuclei, several quantities of fundamental importance were defined. From HF, it is possible to define and justify concepts of chemical reactivity such as the electronic chemical potential (μ), the absolute hardness (η), and the global electrophilicity (ω).The chemical potential μ of the electrons (the negative of the electronegativity χ) is given by

$$\mu = \left(\frac{\partial E}{\partial N}\right)_{v(r)} \quad (5)$$

$$\mu = -\frac{1}{2}(I + A) \quad (6)$$

and has the same value everywhere. In a finite-difference approximation:

$$\chi = -\mu = \frac{1}{2}(I + A) \quad (7)$$

whereI and A are the ionization potential and electron affinity. The change of μ with the number of electrons was defined by Parr and Pearson as a measure for the "absolute hardness" as

$$\eta = \frac{1}{2}\left(\frac{\partial \mu}{\partial N}\right)_{v(r)} = \frac{1}{2}\left(\frac{\partial^2 E}{\partial N^2}\right)_{v(r)} \quad (8)$$

The corresponding finite-difference formula is

$$\eta = \frac{1}{2}(I - A) \quad (9)$$

The electrophilicity index was estimated as previously suggested [30]:

$$\omega = \frac{\mu^2}{2\eta} \quad (10)$$

The calculated I and A values for DCDNB is close to those obtained values. Hence, the substitution of chloro and nitro substituent did not lead to significant changes of the electronegativity and hardness. The electronic chemical potential has the same quantization property as the macroscopic chemical potential.

If free flow is allowed, electrons go from a region of high chemical potential to a region of low chemical potential, until both regions have the same chemical potential value [31]. The larger the difference in chemical potential between two molecules, the easier the reaction will be [32]. As it seen from Table 7, among the series of the systems studied, only ortho-derivatives have lower electronegativity values with respect to DCDNB.

It is generally accepted that a variety of acid-base reactions can be described by the principle: "Hard likes hard and soft likes soft". In agreement with this principle, it is expected that chloro and nitro substituted DCDNB will prefer to react with compound having the different η value (Table 7). The hardness of the systems studied increase in the order. The softness is reciprocal of the hardness. Another useful reactivity descriptor is the elecrophilisity index ω.

8. UV-Vis Spectral Studies

The UV-Vis spectra of DCDNB molecule recorded in methanol solution are given in Fig 5. In an attempt to understand the nature of electronic transitions in terms of their energies and oscillator strengths, HF calculations involving configuration interaction between the singly excited electronic states were conducted on the molecule. Position and absorbance of the experimental peaks together with the calculated transition energies, optical strengths, main configurations and mixing coefficients of the singlet ground and excited states and spectral assignments are given in Table 8. A close agreement has been obtained between the experimental and calculated values of transition energies. HF method with 6-311+G(d,p) basis set calculations predict three transitions in the near ultraviolet region for title molecule. The strong transitions at 516(0.0883), 333.84 (0.0468) and 274.75 (0.0354) nm have been observed at 510, 335 and 283 nm and are assigned to a π–π⁄ transition. The numbers in parentheses represent oscillator strengths.

9. NMR Spectral Analysis

The ^{13}CNMR and^{1}H NMR chemical shifts calculated using gauge including atomic orbital (GIAO) of the DCDNB werecarried out using HF method with 6-311++G(d,p) basis set. The GIAO method is one of the most common approaches for calculating isotropic nuclear magnetic shielding tensors. The NMR spectra calculations were performed by the Gaussian 09Wsoftwarepackage.

Experimental and theoretical chemical shifts of DCDNB in ^{13}CNMR and^{1}H NMR spectra were recorded and the obtained data are presented in Table 9. The observed ^{13}C NMR and ^{1}H NMR spectra of the compound DCDNB are given in the Fig. 6. ^{1}Hatom is mostly localized on periphery of the molecules and their chemical shifts would be more susceptible to intermolecular interactions. Aromatic carbons give signals with chemical shift values from 100 to 200 ppm [33,34]. The observed experimental chemical shift positions of ring carbons of DCDNB lie in the range 142–80ppm. The cumulative effect of nitrogen and chlorine in the hetero ring of DCDNB reduces the electron density of the carbon atom C6, thus its NMR signal is observed in the very downfield at 142 ppm. Due to the influence of electronegative Cl and NO2 atoms and the deshielding effect the chemical shift value of C1 and C2 are also attributed to the downfield NMR signals. The carbon atoms C3, C4 and C5 are significantly observed in the up field with chemical shift values 128, 132 and 140 ppm reveals that the influences of the electronegative nitrogen and chlorine atoms are negligibly small and their signal are observed in the normal range.

^{1}H chemical shifts of DCDNB were obtained by complete analysis of their NMR spectra and interpreted critically in an attempt to quantify the possible different effects actingon the shielding constant of protons. The hydrogen atoms H11 and H16 present in the benzene ring shows NMR peaks in the normal range of aromatic hydrogen atoms and are assigned to 7.2 and 8.2 ppm. The protons are located on the periphery of the molecule and thus are supposed to be more susceptible to molecular solute–solvent effects than the carbon atoms and usually the agreement between the experimental and calculated shifts for ^{1}H is slightly deviated than that of ^{13}C [35].

Conclusion

In the present work, the analyses have been made for vibrational pattern of FT-IR and FT-Raman, UV and NMR spectra. The fundamental frequencies are assigned and the computational calculations are performed by HF method with 6-311+G(d,p) and 6-311++G(d,p)basis sets. The distortion of the structure of the compound due to the substitutions of Cl and NO2 is discussed in detail. The excellent agreement of the calculated and observed vibrational spectra reveals the advantages of 6-311++G(d,p) basis set for quantum chemical calculations. The NLO properties of first order hyperpolarize ability to title component are discussed.

References

[1] G. Booth, Nitro compounds, aromatic, in: Ullmann's Encyclopediaof Industrial Chemistry, John Wiley & Sons, New York, 2007.
[2] A. Bhattacharya, V.C. Purohit, V. Suarez, R. Tichkule, G. Parmer, F. Rinaldi,One-step reductive amidation of nitro arenes: application in the synthesisof acetaminophen, Tetrahedr. Lett. 2006; 47 (11): 1861–1864.
[3] W. Domalewski,L. Stefaniak,G.A. Webb,Journal of Molecular Structure 1993; 295: 19–23.
[4] M.A. Palafox, F.J. Melendez, Journal of Molecular Structure (Theochem) 2003; 625: 17–21.
[5] Q.G. Huang, L.R. Kong, Y.B. Liu, L.S. Wang, Relationships Between Molecular Structure and Chromosomal Aberrations in Vitro Human Lymphocytes Induced by Substituted Nitrobenzene, 1996.
[6] D.N. Shin, J.W. Hahn, K.H. Jung, T.K. Ha, Journal of Raman Spectroscopy 1998; 29: 245–249.
[7] T. Ziegler, Chemical Review 1991; 91: 651–667.
[8] C.E. Blom, C. Altona, Molecular Physics 1976; 31: 1377.

[9] M.J. Frisch et al., Gaussion 09W Program, Gaussian, Inc., Wallingford, CT, 2004.
[10] P. Pulay, G. Fogarasi, G. Pongor, J.E. Boggs, A. Vargha, Journal of American Chemical Society 1983; 105: 7037–7047.
[11] G. Rauhut, P. Pulay, Journal of Physical Chemistry 1995; 99: 3093–3100.
[12] G. Fogarasi, P. Pulay, in: J.R. Durig (Ed.), Vibrational Spectra and Structure (Chapter3), Elsevier, Amsterdam, 1985; 14: 125–130.
[13] G. Fogarasi, X. Zhou, P.W. Taylor, P. Pulay, Journal of American Chemical Society 1992; 114: 8191–8201.
[14] T. Sundius, Journal of Molecular Structure 1990; 218: 321–326.
[15] (a) T. Sundius, Vibirational Spectroscopy 2002; 29: 89–95;
(b) Molvib (V.7.0): Calculation of Harmonic Force Fields and Vibrational Modesof Molecules, QCPE Program No. 807, 2002.
[16] G. Keresztury, J.M. Chalmers, P.R. Griffiths (Eds.), Raman Spectroscopy: Theory in Hand Book of Vibrational Spectroscopy, John Wiley & Sons Ltd., New York, 2002; 1.
[17] G. Keresztury, S. Holly, G. Besenyei, J. Varga, A.Y. Wang, J.R. Durig, Spectrochimica Acta Part A 1993; 49: 2007–2026.
[18] D.C. Young, Computational Chemistry: A Practical Guide for Applying Techniques to RealWorld Problems (Electronic), John Wiley & Sons Inc., New York, 2001.
[19] V. Krishnakumar, N. Prabavathi, Spectrochimica Acta Part A 2009; 72: 738–742.
[20] G. Socrates, Infrared and Raman Characteristic Group Frequencies –Tables andCharts, 3rd edition, John Wiley & Sons, Chichester, 2001.
[21] E. Gladis Anitha, S. Joseph Vedhagiri, K. Parimala, Spectrochimica Acta Part A 2015; 136: 1557–1568.
[22] G. Varsanyi, Vibrational Spectra of Benzene Derivatives, Academic Press, New York, 1969.
[23] D.N. Sathyanarayana, Vibrational Spectroscopy Theory and Application, New Age International Publishers, New Delhi, 2004.
[24] S.P. Saravanan, A. Sankar, K. Parimala, Journal of Molecular Structural 2017; 1127: 784–195.
[25] V. Balachandran, K.Parimala, Journal of molecular structure 2012; 1007: 136–145.
[26] E. Gladis Anitha, S. Joseph Vedhagiri, K. Parimala, SpectrochimicaActa Part A 2015; 136: 1557–1568.
[27] D.A. Kleinman, Physical Review 1962; 126: 1977–1979.
[28] R.S. Mulliken, Journal of Chemical Physics 1995; 23: 1833–1840.
[29] (a) R.G. Parr, W. Yang, Journal of American Chemical Society 1984; 106: 4049–4050.
(b) W. Yang, R.G. Parr, R. Pucci, Journal of Chemical Physics 1984; 81: 2862–2863
[30] R.G. Parr, L.V.Szentpály, S. Liu, Journal of American Chemical Society1999; 121:1922–1924.
[31] R.G. Parr, R.A. Donnelly, M. Levy, W.E.Palke, Journal of Chemical Physics 1978; 68: 3801–3807.
[32] Y. Li, J.N.S. Evans, Journal of American Chemical Society 1995; 117: 7756–7759.
[33] H.O. Kalinowski, S. Berger and S. Braun, Carbon–13 NMR spectroscopy, John Wiley & Sons, Chichester, 1988.
[34] K. Pihlaja, E. Kleinpeter (Eds.), Carbon–13 chemical shifts in Structural and Sterochemical Analysis, VCH Publishers, Deerfield Beach, 1994.
[35] B. Osmiałowski, E. Kolehmainen, R. Gawinecki, Magnetic Resonance in Chemistry 2001; 39: 334–340.

Table 1: Optimized geometrical parameters for DCDNB calculated at HF method with 6-311+G(d,p) and 6-311++G(d,p) basis bets

Bond lengths	6-311+G (d,p)	6-311++G (d,p)	Bond angles	6-311+G (d,p)	6-311++G (d,p)	Dihedral angles	6-311+G (d,p)	6-311++G (d,p)
C1–C2	1.4627	1.4623	C2–C1–C6	118.900	118.889	C6–C1–C2–C3	13.055	13.029
C1–C6	1.3304	1.3303	C2–C1–Cl7	120.880	120.853	C6–C1–C2–N8	–161.065	–160.870
C1–Cl7	1.7234	1.7232	C6–C1–Cl7	120.195	120.232	C17–Cl–C2–C3	–165.176	–165.173
C2–C3	1.4637	1.4632	C1–C2–C3	116.996	177.040	C17–C1–C2–N8	20.702	20.927
C2–N8	1.2914	1.2914	C1–C2–N8	125.087	125.023	C2–C1–C6–C5	–1.336	–1.346
C3–C4	1.4466	1.4465	C3–C2–C4	119.996	119.995	C2–C1–C6–H16	179.894	179.927
C3–N11	1.2823	1.2822	C2–C3–N11	118.686	118.689	Cl7–C1–C6–C5	176.907	176.867
C4–C5	1.3279	1.3279	C4–C3–N11	121.316	121.314	Cl7–Cl–C6–H16	–1.861	–1.858
C4–H14	1.0709	1.0708	C3–C4–C5	117.489	117.481	Cl–C2–C3–C4	–18.083	–18.002
C5–C6	1.4615	1.4617	C3–C4–H14	118.776	118.759	C1–C2–C3–N11	161.716	161.869
C5–Cl15	1.7295	1.7294	C5–C4–H14	123.705	123.730	N8–C2–C3–C4	156.486	156.357
C6–H16	1.0718	1.0717	C4–C5–C6	122.786	122.789	N8–C2–C3–N11	–23.713	–23.770
N8–O9	1.2009	1.2008	C4–C5–Cl15	120.890	120.906	C1–C2–N8–O9	2.001	2.032
N8–O10	1.3851	1.3847	C6–C5–Cl15	116.294	116.274	Cl–C2–N8–O10	175.612	175.617
N11–O12	1.3839	1.3837	C1–C6–C5	121.544	121.535	C3–C2–N8–O10	1.526	1.753
N11–O13	1.2168	1.2167	C1–C6–H16	120.114	120.134	C2–C3–C4–C5	10.871	10.772
			C5–C6–H16	118.330	118.318	C2–C3–C4–H14	–170.999	–171.832
			C2–N8–O9	132.533	132.495	N11–C3–C4–C5	–168.923	–169.096
			C2–N8–O10	113.667	113.705	N11–C3–C4–H14	9.206	9.042
			O9–N8–O10	113.537	113.534	C2–C3–N11–O12	–3.325	–3.467
			C3–N11–O12	113.133	113.089	C2–C3–N11–O13	–178.676	–178.802
			C3–N11–O13	131.282	131.325	C4–C3–N11–O12	176.470	176.402
			O12–N11–O13	115.439	115.44	C4–C3–N11–O13	1.120	1.067
						C3–C4–C5–C6	1.454	1.508

						C3–C4–C5–Cl15	179.457	179.437
						H14–C4–C5–C6	–176.57	–176.529
						H14–C4–C5–Cl15	1.429	1.399
						C4–C5–C6–C1	–6.514	–6.513
						C4–C5–C6–H16	172.276	172.234
						Cl15–C5–C6–C1	175.396	175.468
						Cl15–C5–C6–H16	–5.812	–5.783

Table 2: Definition of internal coordinates for DCDNB.

Sl.No	Type	Symbol	Definition
Stretching			
1–6	P_i	C–C	C1–C2, C2–C3, C3–C4,C4–C5, C5–C6, C6–C1
7–8	q_i	C–H	C4–H14,C6–H16
9–10	D_i	C–Cl	C1–Cl7,C5–Cl15
11–12	Q_i	C–N	C2–N8,C3–N11
13–16	r_i	N–O	N8–O9,N8–O10 N11–O12, N11–O13
Bending			
17–22	α_i	Ring	C1–C2–C3, C2–C3–C4, C3–C4–C5, C4–C5–C6, C5–C6–C1, C6–C1–C2
23–26	β_i	CCH	C3–C4–H14, C5–C4–H14, C5–C6–H16, C1–C6–H16
27–30	υ_i	CCl	C2–C1–Cl7, C6–C1–Cl7, C4–C5–Cl15, C6–C5–Cl15
31–34	σ_i	CCN	C1–C2–N8, C3–C2–N8 C2–C3–N11, C4–C3–N11
35–38	γ_i	CNO	C2–N8–O9, C2–N8–O10, C3–N11–O12, C3–N11–O13
39–40	σ_i	ONO	O9–N8–O10, O12–N11–O13
Out-of-Plane bending			
41–42	ω_i	CCCH	H14–C4–C5–C3, H16–C6–C1–C5
43–44	ω_i	CCCl	Cl7–C1–C6–C2, Cl15–C5–C4–C6
45–46	ψ_i	CCCN	N8–C2–C1–C3, N11–C3–C4–C2
Torsion			
47–52	τ_i	tRing	C1–C2–C3–C4, C2–C3–C4–C5, C3–C4–C5–C6, C4–C5–C6–C1, C5–C6–C1–C2, C6–C1–C2–C3
53–54	τ_i	tNO2	C2–N8–O9–O10, C3–N11–O12–O13

Table 3: Definition of local coordinates for DCDNB.

No(i)	Symbol	Definition
1–6	νCC	P1, P2, P3, P4, P5, P6
7–8	νCH	q7, q8
9–10	νCCl	D9, D10
11–12	νCN	Q11, Q12
13–14	NO2sym	(r13+r14)/√2, (r15+r16)/√2
15–16	NO2asym	(r13–r14)/√2, (r15–r16)/√2
17	Rtrigd	(α17–α18+α19–α20+α21–α22)/√6
18	Rsymd	(–α17–α18+2α19–α20–α21+2α22)/√12
19	Rasymd	(α19–α20+α21–α22)/√2
20–21	bCH	(β23–β24)/√2, (β25–β26)/√2
22–23	bCCl	(υ27– υ28)/√2, (υ29– υ30)/√2
24–25	bCN	(γ31– γ32)/√2, (γ33– γ34)/√2
26–27	NO_2 twist	(γ35+γ36)/√2, (γ37+γ38)/√2
28–29	NO_2 rock	(γ35–γ36)/√2, (γ37–γ38)/√2
30–31	NO_2sciss	(σ39–γ35–γ36)/√2, (σ40–γ37–γ38)/√2
32–33	γCCH	ω41, ω42
34–35	γCCCl	ω43, ω44
36–37	γCCN	ψ45, ψ46
38	tRtrigd	(τ47+τ48+τ49+τ50+τ51+τ52)/√6
39	tRsymd	(τ47+τ49+τ50+τ52)/2
40	tRasymd	(–τ47+2τ48–τ49–τ50+2τ51–τ52)/√12
41–42	NO2wagg	τ53, τ54

Table 4: The observed FT-IR, FT-Raman and calculated frequencies using HF/6-311+G(d,p) and HF/6-311++G(d,p) force field along with their probable assignments of DCDNB.

No.	Observed wavenumbers		Calculated wavenumbers				[a]Vibrational Assignments
			6-311+G(d,p)		6-311++G(d,p)		
	FT-IR	FT-Raman	Unscaled	Scaled	Unscaled	Scaled	
1	3400(w)		3399	3211	3391	3205	νCH(99)
2	3250(w)	2750(w)	3384	3203	3382	3201	νCH(99)
3	1950(vw)		1840	1793	1831	1785	NO2asym(89)
4	1800(w)		1818	1742	1811	1736	NO2asym(87)
5			1746	1659	1735	1651	νCC(84)
6	1700(s)		1733	1639	1732	1633	νCC(82)
7	1600(s)		1558	1525	1559	1523	NO2sym(80)
8	1550(w)		1544	1512	1535	1512	NO2sym(78)
9	1450(vw)	1400(s)	1469	1439	1463	1431	νCC(71)
10			1417	1397	1412	1396	νCC(65)
11	1300(s)		1364	1324	1354	1318	βCH(63), Rtrigd(41)
12	1250(vs)	1250(vs)	1252	1216	1242	1212	βCH(58), Rsymd(32)
13			1228	1193	1227	1186	νCC(54)
14			1174	1152	1168	1143	νCC(49)
15	1150(w)	1150(w)	1154	1138	1153	1127	νCN(58), βCH(32)
16	1035(vw)		1095	1073	1082	1065	νCN(51), βCCl(29)
17	1010(vw)		993	978	991	964	νCCl(46), νCN(27), βCH(22)
18		980(w)	983	961	976	958	Rtrigd(46),νCH(29), νCCl(14)
19			964	652	963	647	Rasymd(40), βCN(13),νCCl(11)
20			907	891	902	885	νCCl(38), Rtrigd(21), βCH(18)
21			823	814	827	804	NO2 sciss(65)
22			786	762	781	757	NO2 sciss(58)
23		750(s)	754	725	746	715	NO2 rock(48)
24	700(s)		703	695	689	689	Rsymd(39), βCCl(24),νCN(15)
25		680(vw)	677	642	672	638	NO2 rock(42)
26	650(s)		651	628	643	617	tRtrigd(36),γCH(14), γCCl(12)
27			608	591	598	584	γCH(31),tRtrigd(31), γCCl(12)
28			590	575	589	568	γCH(33), tRtrigd(24)
29		550(vw)	569	542	561	531	tRasym(39),γCCl(38)
30	510(w)		503	491	492	489	tRsymd(29),γCCl(26),γCN(11)
31	480(vw)		475	462	463	457	βCCl(28), Rsymd(36),βCH(12)
32		450(vw)	451	443	442	435	βCN(27), νCCl(36),βCH(12)
33		400(s)	381	374	375	368	NO2wagg(44), γCN(20)
34		350(s)	358	341	351	337	βCN(37), βCH(36),νCCl(12)
35		300(s)	315	302	308	297	NO2wagg(34), βCN(20)
36		250(vw)	292	284	283	276	βCCl(27),νCC(36), βCN(12)
37			213	205	208	199	γCCl(20), Rsymd(17),νCN(13)
38			200	189	192	179	γCCl(46), tRsymd(18), γCH(15)
39		180(vw)	188	174	181	168	γCN(36),tRasymd(18),γCH(15)
40			130	121	122	117	γCN(31), tRsymd(18), γCCl(15)
41			119	108	112	101	NO2 twist(38)
42			59	45	43	38	NO2 twist(23)

[a]Only contributions larger than 10% are given. Experimental relative intensities are abbreviated as follows: vs-very strong, s-strong, m-medium, w-weak, vw-very weak. Abbreviations; ν-stretching, sym-symmetric stretching, asym-asymmetric stretching, b-bending, d-deformation, R-ring, sciss-scissoring, rock- rocking, wagg-wagging, twist-twisting, β- in-plane bending, γ- out-of-plane bending, t-torsion, trig-trigonal.

Table 5: Electric dipole moment (Debye), average polariability($\alpha_0\times10^{-24}$esu), first hyper polarizability ($\beta_0\times10^{-24}$esu) for DCDNB calculated by HF with 6-311+G(d,p) and 6-311++G(d,p) basis sets.

Parameters	6-311+G(d,p)	6-311++G(d,p)	Parameters	6-311+G(d,p)	6-311++G(d,p)
μ_x	–3.6131	–3.6100	β_{xxx}	–7.2031	–7.0538
μ_y	1.5410	1.5445	β_{xxy}	–7.047	–6.9649
μ_z	–0.1569	–0.1670	β_{xyy}	–22.29	–22.319
μ	23.79	23.54	β_{yyy}	44.78	44.874
α_{xx}	–99.240	–99.221	β_{xxz}	6.564	–6.5919
α_{xy}	–1.485	1.4575	β_{xyz}	–5.377	–5.4130
α_{yy}	105.646	–105.651	β_{yyz}	4.982	4.8930
α_{xz}	–1.452	–1.4654	β_{xzz}	8.997	8.9770
α_{yz}	–3.930	–3.912	β_{yzz}	–2.417	–2.4572
α_{zz}	–93.353	–93.361	β_{zzz}	0.7054	0.7194
α_0	–99.413	–99.313	β_0	1.668	1.662

Table 6: Muliken atomic charges are calculated by HF method with 6-311+G(d,p) and 6-311++G(d,p) basis sets for DCDNB

Atoms	6-311+G(d,p)	6-311++G(d,p)	Atoms	6-311+G(d,p)	6-311++G(d,p)
C1	2.289	1.495	O9	–0.037	–0.084
C2	–1.575	–1.479	O10	0.258	0.255
C3	–0.083	–0.082	N11	–0.380	–0.357
C4	–0.374	0.458	O12	0.225	0.230
C5	1.177	0.457	O13	–0.094	–0.100
C6	–2.138	–1.163	H14	0.199	0.311
Cl7	0.299	0.332	Cl15	0.342	0.383
N8	–0.316	–0.232	H16	0.206	0.294

Table 7: Calculated at the HF/6-311+G(d,p) of ionization potential (I, a.u), vertical ionization energy (A, a.u), HOMO (H) and LUMO (L) values (a.u), electronic chemical potential (μ, a.u), global hardness (η, a.u), global softness (S, a.u), elecronegativity (χ, a.u), electrophilisity indices (ω, a.u) for DCDNB.

Chemical parameters	Calculated values
I	–0.021
A	0.019
HOMO	–0.236
HOMO–1	–0.265
LUMO	–0.037
LUMO+1	–0.021
Δ(HOMO–LUMO)	–0.213
μ	–0.025
η	0.005
S	–232.483
χ	0.024
ω	0.045

Table 8: Experimental and calculated absorption wavelength (nm), excitation energies (eV), oscillator strength (f) of DFDNB by HF/6-311+G(d,p) method.

Excitation states	Excitation energies (eV)	Wavelength (nm)		Oscillator strength (f)
		Experimental	Theoretical	
1	2.6513	510	516.00	0.0883
2	3.6585	335	333.84	0.0468
3	3.8997		312.29	0.0053
4	3.9962		360.45	0.0072
5	4.4027	283	274.75	0.0354
6	4.641		258.69	0.0048

Table 9: The experimental and calculated ^{13}C and ^{1}H NMR isotropic chemical shifts (δin ppm) of DFDNB by HF/6-311+G(d,p) level of theory

Atoms	Experimental	Theoretical
C1	0.5	114.15
C2	80	111.36
C3	128	115.46
C4	132	138.67
C5	140	152.18
C6	142	155.72
H11	7.2	7.5
H16	8.2	8.5

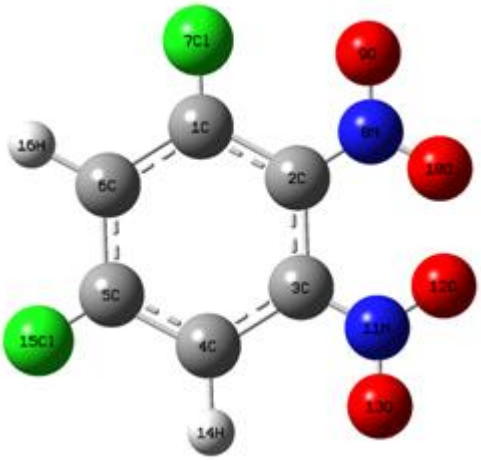

Figure 1: Molecular structure of DCDNB with atom numbering

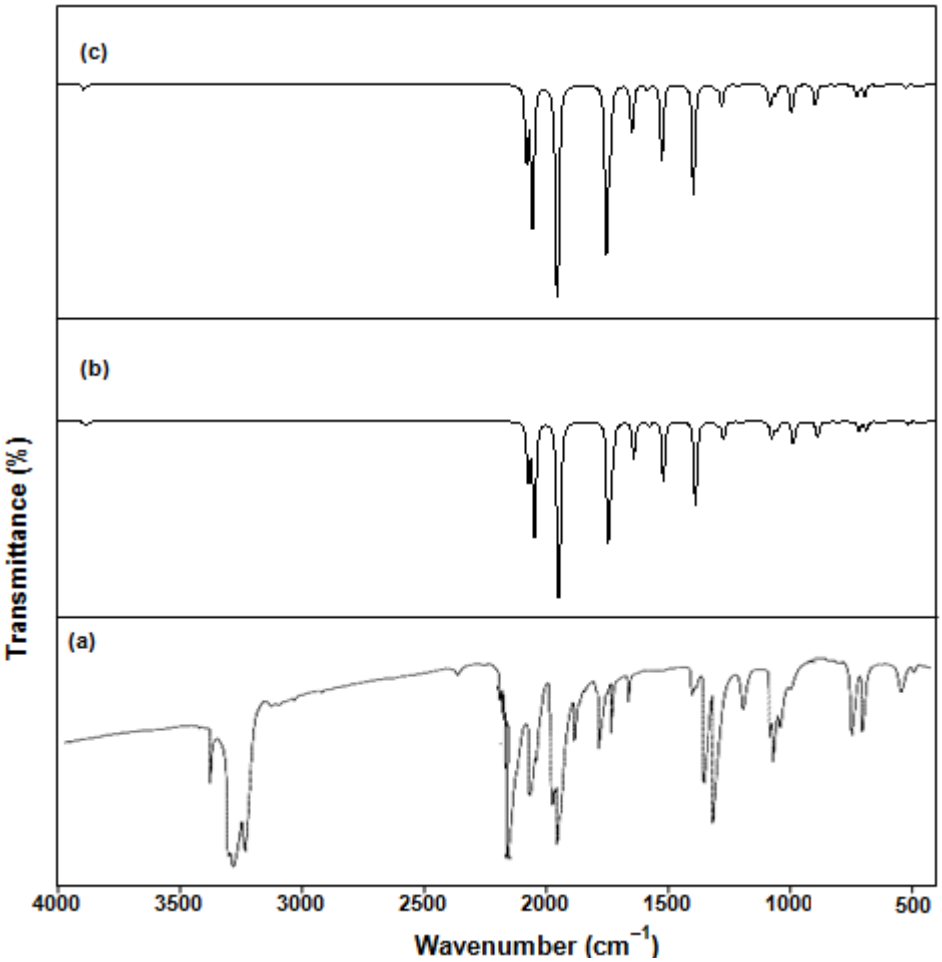

Figure 2: FT-IR spectra of DCDNB (a) observed (b) calculated with HF/6-311+G(d,p) and (c) calculated with HF/6-311++G(d,p)

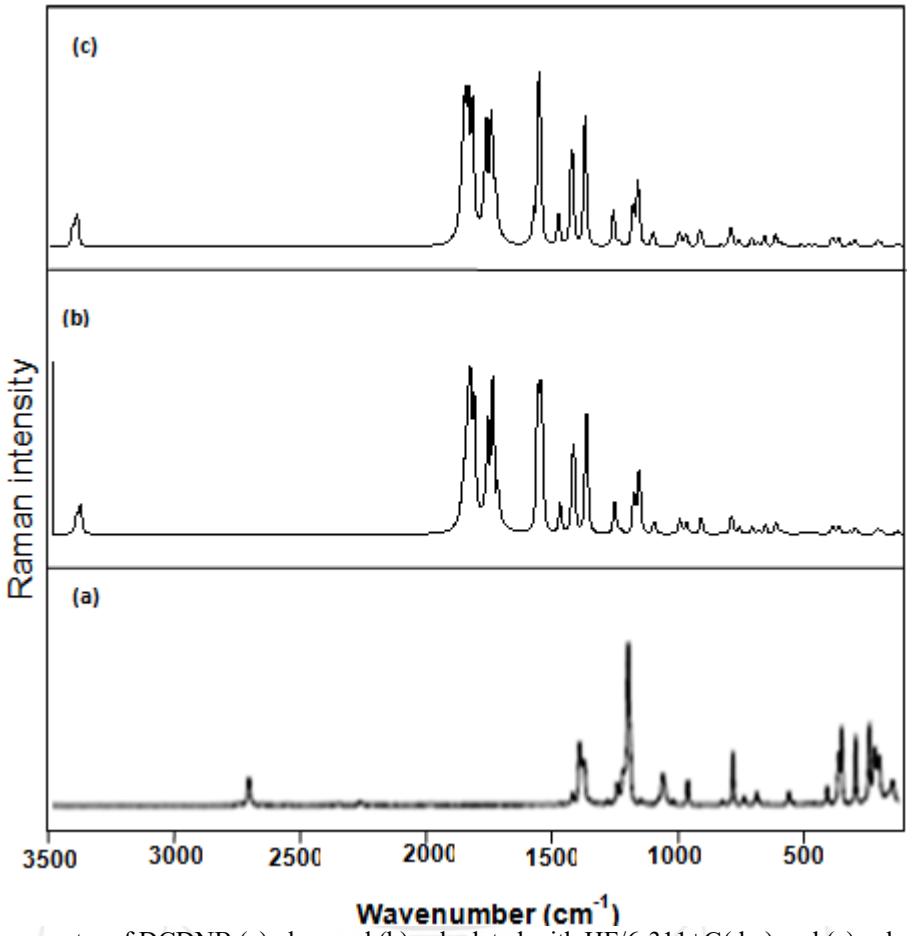

Figure 3: FT-Raman spectra of DCDNB (a) observed (b) calculated with HF/6-311+G(d,p) and (c) calculated with HF/6-311++G(d,p).

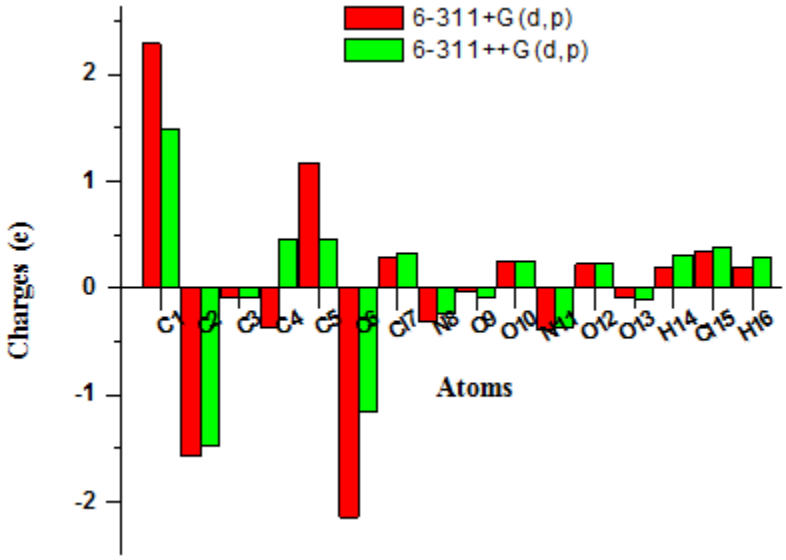

Figure 4: Mulliken charge distributions of DCDNB molecule

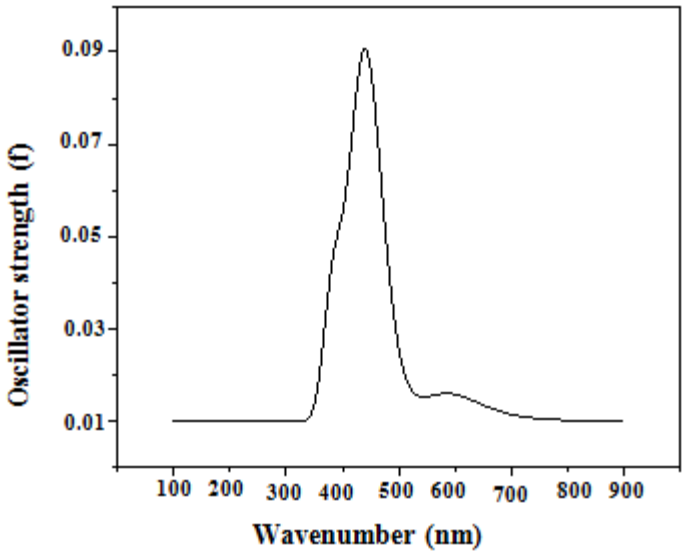

Figure 5: UV-Vis spectrum of DCDNB

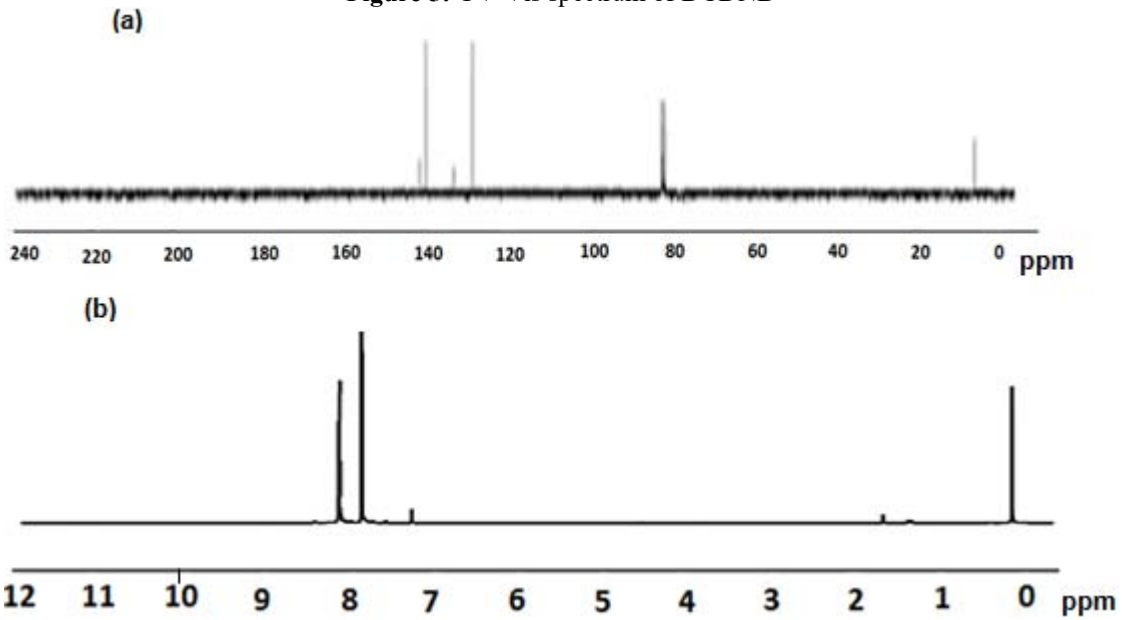

Figure 6: Experimental (a) ^{13}C and (b) ^{1}H and NMR chemical shifts of DCDNB compound